Clinical, genotypic, and imaging characterization of the spectrum of ABCA4 retinopathies

Romano, F.; Lamanna, F.; Boon, C.J.F.; Siligato, A.; Kalra, G.; Agarwal, A.; ... ; Salvetti, A.P.

AMERICAN ACADEMY OF OPHTHALMOLOGY®

Clinical, Genotypic, and Imaging Characterization of the Spectrum of *ABCA4* Retinopathies

Francesco Romano, MD,[1,2] Francesca Lamanna, MD,[1] Camiel J.F. Boon, MD, PhD,[3,4] Alessandro Siligato, MD,[1] Gagan Kalra, MD,[5] Aniruddha Agarwal, MD,[6] Chiara Medori, MSc,[7] Matteo Bertelli, MD,[7] Marco Pellegrini, MD,[1] Alessandro Invernizzi, MD,[1,8] Giovanni Staurenghi, MD,[1] Anna Paola Salvetti, MD[1]

Purpose: To investigate the clinical and genotypic differences in the spectrum of *ABCA4*-associated retinopathies (ABCA4Rs).

Design: Observational, cross sectional case series.

Participants: Sixty-six patients (132 eyes) carrying biallelic *ABCA4* variants.

Methods: Patients underwent visual acuity measurement and multimodal imaging. Clinical records were reviewed for age at onset, presenting symptoms, genetic variants, and electroretinogram (ERG). Each eye was assigned to a phenotype based on age at onset, imaging and ERG: cone dystrophy-bull's-eye maculopathy (CD-BEM, 40 eyes), cone-rod dystrophy (CRD, 12 eyes), Stargardt disease (SD, 28 eyes), late-onset SD (LO-SD, 38 eyes), and fundus flavimaculatus (14 eyes). Images were analyzed for: peripapillary sparing, retinal pigment epithelium (RPE) atrophy (definitely decreased autofluorescence, DDAF), flecks patterns using autofluorescence; type of atrophy according to Classification of Atrophy Meeting reports, macular and choroidal thickness on OCT; and choriocapillaris flow deficits on OCT angiography.

Main Outcome Measures: Primary outcome was to report the demographic, genotypic, and imaging characteristics of the different ABCA4R phenotypes. Secondary objectives included the assessment of imaging biomarkers as outcome measures for clinical trials.

Results: Age at onset was lower in CRD (12 $\pm$ 8 years) and higher in patients with LO-SD (59 $\pm$ 9 years) (all $P < 0.01$). Central vision loss was a common presenting symptom in CD-BEM and SD, whereas patients with LO-SD primarily complained of difficult dark adaptation. Missense variants were more frequent in CD-BEM, and splice site in CRD and LO-SD ($P < 0.05$). Peripapillary sparing was absent in 3 eyes with LO-SD (8%). Cone dystrophy-bull's-eye maculopathy eyes typically had complete outer retinal atrophy alterations (98%), whereas CRD and SD eyes showed both complete outer retinal atrophy and complete RPE and outer retinal atrophy (cRORA) (71%−100%). Patients with LO-SD had larger areas of DDAF (100% cRORA) and of choriocapillaris flow deficits (all $P < 0.01$). Repeatability of DDAF measurements was low for some phenotypes (CD-BEM and CRD) and atrophic areas <7.5 mm^2. Resorbed flecks were significantly associated with CRD and LO-SD ($P < 0.01$).

Conclusions: This research provides a thorough evaluation of the spectrum of ABCA4R. Our findings suggest that certain phenotypes show preferential photoreceptor degeneration (e.g., CD-BEM), whereas others have substantial RPE and choriocapillaris alterations (e.g., LO-SD). We recommend that clinical trial end points take into consideration these imaging features to improve the interpretation of their results.

Financial Disclosure(s): Proprietary or commercial disclosure may be found in the Footnotes and Disclosures at the end of this article. *Ophthalmology Retina 2024;8:509-519 © 2023 by the American Academy of Ophthalmology*

Supplemental material available at www.ophthalmologyretina.org.

ABCA4-related retinopathies (ABCA4Rs) are the most common monogenic retinal dystrophies, affecting an estimated 1 in 6578 individuals.[1] Biallelic mutations in *ABCA4* gene result in a variable degree of function loss of the encoded photoreceptor transmembrane rim protein ATP-binding cassette transporter (ABCR), leading to the abnormal accumulation of bisretinoids and subsequent degeneration of the outer retina and retinal pigment epithelium (RPE).[2,3]

ABCA4-related retinopathy phenotypes encompass a broad spectrum of clinical presentations including Stargardt disease (SD), fundus flavimaculatus (FFM), bull's-eye maculopathy, cone-rod dystrophy (CRD) and even a retinitis pigmentosa-like phenotype, with progressive or stationary

https://doi.org/10.1016/j.oret.2023.10.023
ISSN 2468-6530/23

course.[4] Different classifications based on the extent of flecks and macular atrophy, autofluorescence patterns, and electrophysiology have been proposed over the last decades.[5–8]

However, ABCA4R phenotypes are quite heterogeneous and may not always conform to a single imaging or electrophysiological pattern. This aspect poses a challenge when interpreting results from clinical trials, particularly in the absence of long-term natural history studies.[7] The accuracy of the current outcome measures remains a matter of debate in literature, with the principal parameters being definitely decreased autofluorescence (DDAF), quantitative autofluorescence, outer nuclear layer, and ellipsoid zone alterations.[9–11] Furthermore, attention has been recently devoted to novel retinal and choroidal biomarkers using a multimodal approach.[12–15]

Considering the critical need for a comprehensive assessment of ABCA4Rs to refine the selection of outcome measures,[16] the aim of this study is to investigate the principal differences across its phenotypes in a large Italian cohort.

Methods

The study was designed as an observational, cross sectional case series and conducted at the Eye Clinic of Ospedale Luigi Sacco (Department of Biomedical and Clinical Sciences, University of Milan, Milan, Italy). The procedures adhered to the tenets of the Declaration of Helsinki, and all patients were enrolled after approval by the institutional review board of Ospedale Luigi Sacco. Written informed consent was obtained from each participant after explaining the study protocol.

The primary outcome of our study is to report the demographic, genotypic, and imaging characteristics of ABCA4R phenotypes. Secondary objectives include the assessment of different imaging biomarkers as outcome measures for these phenotypes.

Patient Selection

We included all consecutive patients presenting at our Inherited Retinal Dystrophy service from January to December 2022 with the following characteristics: (1) detection of biallelic mutations with a maximum of 1 hypomorphic variant in combination with class 4 or 5 variant in *ABCA4* gene (Online Mendelian Inheritance in Man [OMIM] #601691) by an external genetics laboratory using next-generation sequencing of target regions as previously described;[17] (2) a clinical presentation compatible with ABCA4R; (3) age of $\geq$12 years at study visit; and (4) absence of media opacities. We excluded patients with macular neovascularization, refractive errors $>$ $\pm$5 diopters (spherical equivalent), under retinotoxic medications (e.g., hydroxychloroquine), and with any ocular or systemic conditions (e.g., glaucoma, keratoconus, and diabetes) that might affect our analysis.

Study Protocol and Phenotyping

All patients underwent a complete ophthalmic examination, including: best-corrected visual acuity (BCVA) measurement using ETDRS chart; slit-lamp biomicroscopy; pupil dilation using 1.0% tropicamide and 2.5% phenylephrine; color fundus photography of the posterior pole (EIDON; CenterVue); dense OCT macular volumes covering an area of 25° $\times$ 30° (61 lines, automatic real-time tracking = 16 frames) (Spectralis OCT2; Heidelberg Engineering GmbH); swept-source 6 $\times$ 6-mm OCT angiography (OCTA) scan centered on the fovea (PLEX Elite 9000; Carl Zeiss Meditec); and 30° $\times$ 30° and 55° $\times$ 55° blue (488-nm excitation) and near-infrared autofluorescence (787-nm excitation) images using a confocal scanning laser ophthalmoscope (Spectralis HRA2; Heidelberg Engineering).

Clinical notes were reviewed for mutations in the *ABCA4* gene, age and presenting symptoms at clinical onset, and electroretinogram (ERG) alterations. The identified mutations were checked for pathogenicity according to the recommendations of the American College of Medical Genetics and the Association for Molecular Pathology[18] on ClinVar — a public archive for interpreting the clinical significance of human variants (National Center for Biotechnology Information, National Institutes of Health; https://www.ncbi.nlm.nih.gov/clinvar/) — and classified as follows: missense, nonsense, structural (including insertions, deletions, inversions, and copy number variations), and splice site variants. We subdivided presenting symptoms into photosensitivity, abnormal color vision, central vision loss (with or without peripheral visual loss), paracentral scotomas, and impaired dark adaptation.

Each eye was assigned to one of the following phenotypes based on the combination of age at onset, imaging features and ERG:

- cone dystrophy-bull's-eye maculopathy (CD-BEM) — no age restriction, mostly photoreceptors' abnormalities and few flecks confined to the fovea and parafovea, normal scotopic, and full-field ERG with abnormalities only evident on pattern ERG;[19]
- cone-rod dystrophy — age at onset $<$ 45 years, concomitant cone and rod degeneration with cones primarily involved, and abnormal full-field, photopic, and scotopic ERG;[20]
- classic SD — age at onset $<$ 45 years, areas of RPE atrophy and flecks extending to the posterior pole (within and beyond the vascular arcades), and altered pattern ERG with frequent photopic abnormalities;[8]
- late-onset SD (LO-SD) — age at onset of $\geq$45 years, large areas of RPE atrophy with preferential foveal and peripapillary sparing, and variable ERG alterations;[21]
- fundus flavimaculatus — presence of isolated flecks after the second–third decade and no or slightly altered ERG.[22]

Imaging Analysis

All imaging studies were carefully analyzed by 2 independent ophthalmologists with a specific training in medical retina (F.R. and F.L.). Mean values of obtained measurements were used for statistical analysis, and the agreement between the 2 graders was evaluated. Discordant qualitative findings were solved by a third senior grader (A.P.S.).

Normalized blue autofluorescence images were evaluated for peripapillary sparing, size of RPE atrophy, and the presence of flecks. Quantification of RPE atrophy was performed on 30° $\times$ 30° acquisitions using Heidelberg semiautomated software RegionFinder (version 2.6.5.0). Retinal pigment epithelium atrophy was defined as a level of darkness $>$90% that of the optic nerve (considered the reference point for 100% level of darkness) in areas of DDAF.[23] Flecks were categorized into 5 different patterns according to their morphology: punctate, linear, pisciform, multiradiate, and resorbed, after a previous classification proposal.[16] Previous imaging studies were accessed to confirm the presence of hyperautofluorescence flecks and their resorption over time, which appeared as hypoautofluorescent and coalescent lesions at the posterior pole.

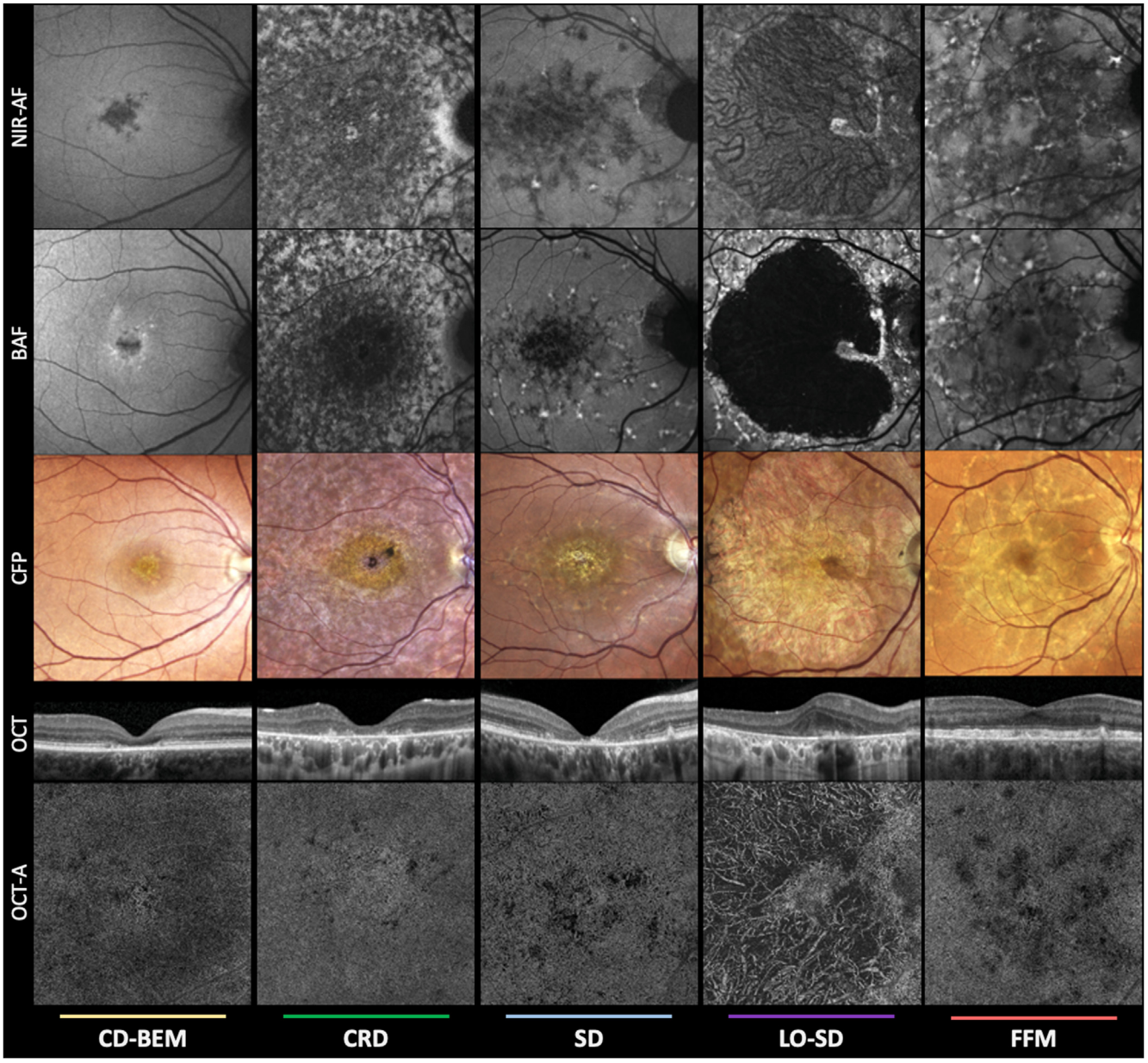

Figure 1. Multimodal imaging characterization of the 5 described phenotypes of *ABCA4*-related retinopathies. Loss of foveal reflex can be observed on fundus photograph of patients affected by cone dystrophy-bull's-eye maculopathy (CD-BEM), which corresponds to hypoautofluorescent areas on near-infrared autofluorescence (NIR-AF) and blue autofluorescence (BAF), with surrounding hyper-autofluorescent flecks. Significant disruption of the outer retinal layers in the foveal and parafoveal areas can be observed on OCT, whereas few small flow deficits can be appreciated at the level of the choriocapillaris in the foveal area. In the cone-rod dystrophy phenotype, diffuse photoreceptor and retinal pigment epithelium (RPE) changes can be seen at and outside the posterior pole. The flecks pattern is mostly the "resorbed" type and appears as hypoautofluorescent using both NIR-AF and BAF imaging. The outer nuclear layer seems significantly thinned on OCT, with some areas of choroidal hypertransmission due to RPE atrophy; flow deficits in the choriocapillaris extend beyond the macular area. The Stargardt phenotype is characterized by profound macular atrophy surrounded by different patterns of yellowish flecks. Retinal pigment epithelium atrophy acquires a hypoautofluorescent pattern on NIR-AF and a granular aspect using BAF due to the accumulation of overlying lipofuscin. On OCT, the ellipsoid zone and external limiting membrane are interrupted in the macula, where some hyperreflective subretinal material accumulates (e.g., flecks or pigment). Choriocapillaris flow deficits are more extensive on 6 × 6-mm macular OCT angiography (OCTA). In late-onset Stargardt disease (LO-SD), large areas of RPE atrophy at the posterior pole with minimal foveal sparing can be observed, surrounded mostly by multiradiate and resorbed flecks. Retinal pigment epithelium atrophy seems hypoautofluorescent using both BAF and NIR-AF techniques and corresponds to areas of complete RPE and outer retinal atrophy on OCT. The choriocapillaris is absent underneath areas of RPE atrophy and slightly preserved at the fovea. Fundus flavimaculatus (FFM) is characterized by diffuse and multifaceted flecks throughout the posterior pole. On autofluorescence imaging, flecks can be hyper-autofluorescent or hypoautofluorescent based on their composition and stage. The outer retinal layers seem thick and elongated, and some choriocapillaris flow deficits can be observed in correspondence with larger flecks. CFP = color fundus photography; CRD = cone-rod dystrophy.

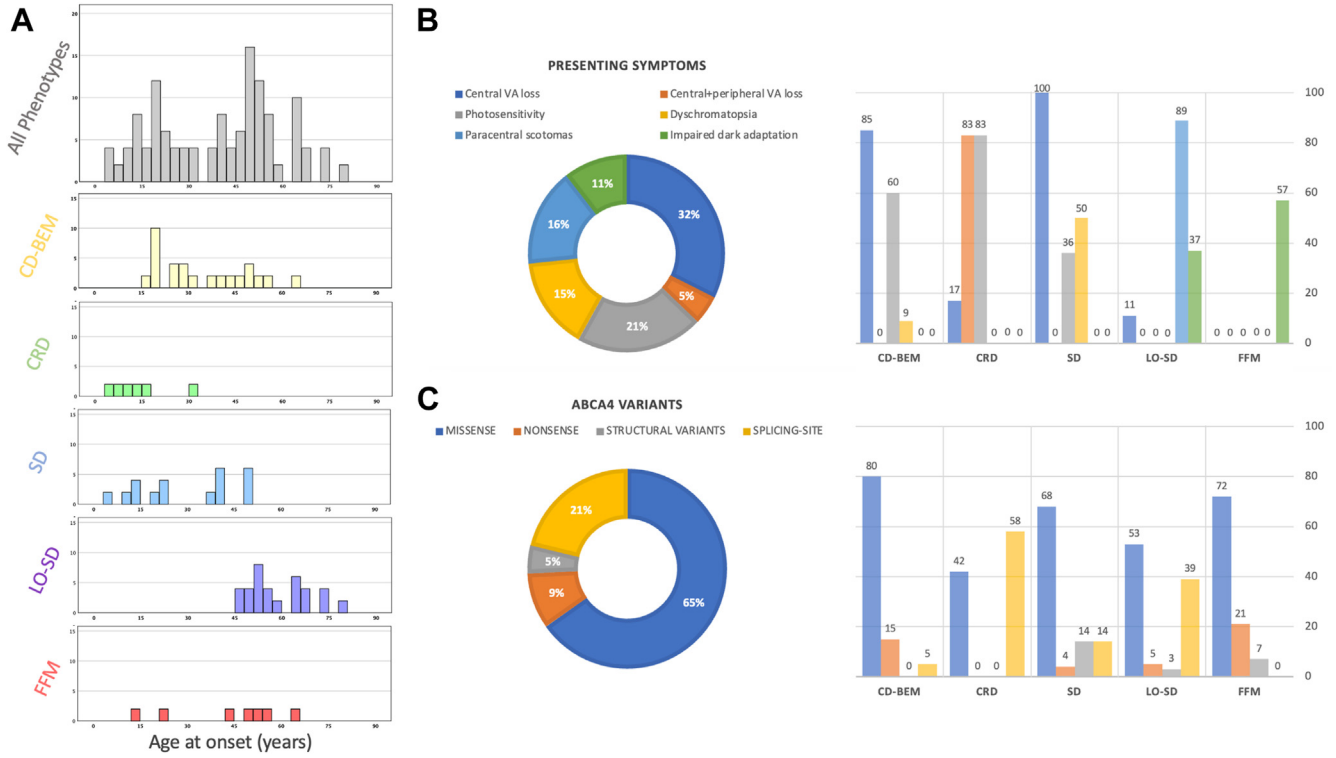

Figure 2. Age at onset, presenting symptoms and variant distribution across the different phenotypes of *ABCA4*-associated retinopathies. **A**, Age at onset seems quite variable in cone dystrophy-bull's-eye maculopathy (CD-BEM), classic Stargardt disease (SD), and fundus flavimaculatus (FFM) phenotypes, whereas it is earlier in the course of cone-rod dystrophy (CRD) and more advanced in patients with late-onset SD (LO-SD). **B**, Presenting symptoms are also different across phenotypes, with central vision loss and photosensitivity being more common in CD-BEM, CRD, and SD, whereas difficult dark adaptation is more frequently associated with LO-SD and FFM. **C**, Missense variants in the *ABCA4* gene are homogeneously distributed in our cohort (42%–80%), whereas splice site variants are more frequent in patients with CRD and LO-SD (58% and 39%, respectively). Structural variants are more commonly observed in patients with SD (14%) than in other phenotypes. VA = visual acuity.

Macular OCT volumes were examined for retinal and choroidal thickness and for grading incomplete and complete outer retinal and RPE and outer retinal atrophy (cRORA) according to the Classification of Atrophy Meeting recommendations.[24] Retinal thickness was quantified automatically after placing an ETDRS grid centered at the fovea using the in-built Spectralis mapping software on Heidelberg Eye Explorer (version 1.10.4.0). Measurements were collected for each of the following subfields or areas: central subfield thickness (the inner 1-mm-diameter circle); parafovea, mean value of the 4 subfields in the inner ETDRS ring (1–3 mm); and perifovea, mean value of the 4 subfields in the outer ETDRS ring (3–6 mm). Subfoveal choroidal thickness was calculated as the distance between the outer margin of the RPE and the hyporeflective sclero-choroidal interface.[25]

OCT angiography scans were analyzed to study choriocapillaris (CC) alterations. In detail, 6 × 6-mm CC angiography and enface slabs were automatically segmented by the software after removal of projection artifacts' and were exported as Tag Image File Format (.tiff) images. Manual correction was permitted in case of significant segmentation errors. Enface slabs were imported to the open-source software FIJI (ImageJ; National Institutes of Health), and areas of RPE atrophy were identified as hyperreflective to create a mask. After applying the mask and excluding areas of RPE atrophy, CC angiography slabs underwent low-contrast binarization using a local thresholding strategy (Phansalkar method).[26] Choriocapillaris rarefaction was expressed as flow deficit (μm^2) — defined as the area of CC greater than intercapillary distance without OCTA signal.[27]

Statistical Analysis

All statistical analyses were performed by means of SPSS software version 28.0 (IBM Corporation). Descriptive statistics are presented as mean ± standard deviation (range), median (quartiles), or frequencies (%).

Differences in clinical, demographic, and genotypic findings among phenotypes were explored with chi-square test or Fisher exact test for categorical variables and analysis of variance adopting *post hoc* Tukey honestly significant difference correction for numerical variables. Significance was set at $P < 0.05$ and all tests were 2-sided. As the 2 eyes within the same subject were highly concordant (100%), both eyes were included for descriptive purposes but only data from the better-seeing eyes were considered for multiple comparisons among phenotypes. Interrater agreement was assessed using intraclass correlation coefficient (95% confidence intervals) and Cohen's k factor (k, 95% confidence intervals). Limits of agreement were visualized using Bland–Altman plots and bar charts.

Table 1. Clinical and Demographic Characteristics of the Studied Cohorts

	All	CD-BEM	CRD	SD	LO-SD	FFM
Patients, n (%)	66	20 (30.3%)	6 (9.1%)	14 (21.2%)	19 (27.8%)	7 (10.6%)
Eyes, n	132	40	12	28	38	14
Age, yr	46.3 + 18.6	41.6 + 14.8	27.5 + 13.7	39.9 + 18.9	63.1 + 10.6	43.6 + 17.3
Sex						
Male, n (%)	32 (48.5%)	13 (65%)	2 (33.3%)	6 (42.9%)	9 (47.4%)	2 (28.6%)
Female, n (%)	34 (51.5%)	7 (35%)	4 (66.7%)	8 (57.1%)	10 (52.6%)	5 (71.4%)
BCVA (ETDRS letters)	50.7 + 22.0	46.2 + 15.4	28.8 + 13.5	37.7 + 11.5	61.6 + 23.6	78.5 + 10.5
(Snellen equivalent)	20/100	20/125	20/240	20/200	20/60	20/25
Age at onset, yr	39.1 + 19.3	33.9 + 14.2	13.8 + 8.6	29.1 + 15.7	58.6 + 9.4	42.4 + 17.7
Presenting symptoms						
Central VA loss, n (%)	34 (51.5%)	17 (85%)	1 (16.7%)	14 (100%)	2 (10.5%)	0 (0%)
Central + peripheral VA loss, n (%)	5 (7.6%)	0 (0%)	5 (83.3%)	0 (0%)	0 (0%)	0 (0%)
Photophobia, n (%)	22 (33.3%)	12 (60%)	5 (83.3%)	5 (35.7%)	0 (0%)	0 (0%)
Dyschromatopsia, n (%)	16 (24.2%)	9 (45%)	0 (0%)	7 (50%)	0 (0%)	0 (0%)
Paracentral scotomas, n (%)	17 (25.8%)	0 (0%)	0 (0%)	0 (0%)	17 (89.5%)	0 (0%)
IDA, n (%)	11 (16.7%)	0 (0%)	0 (0%)	0 (0%)	7 (36.8%)	4 (57.1%)
Asymptomatic, n (%)	3 (4.5%)	0 (0%)	0 (0%)	0 (0%)	0 (0%)	3 (42.9%)

BCVA = best-corrected visual acuity; CD-BEM = cone dystrophy-bull's-eye maculopathy; CRD = cone-rod dystrophy; FFM = fundus flavimaculatus; IDA = impaired dark adaptation; LO-SD = late-onset Stargardt disease; SD = Stargardt disease; VA = visual acuity.

Results

Clinical and Demographic Characteristics

A total of 66 patients (132 eyes) with a slight female predominance (34, 51.5%) were enrolled in this study. Based on our assessment, 20 patients were classified as CD-BEM (30.3%), 6 as CRD (9.1%), 14 as SD (21.2%), 19 as LO-SD (28.8%), and 7 as FFM (10.6%) (Fig 1).

Patients with CRD had a significantly younger age of onset compared with all other phenotypes (13.8 ± 8.6 years; all $P \leq 0.01$). Central vision loss was the most common presenting symptom in CD-BEM (85%, $P < 0.001$) and SD (100%, $P < 0.001$), whereas most of the patients with CRD complained of photosensitivity and central visual loss followed by peripheral difficulties (83.3%, $P < 0.001$). In contrast, patients with FFM were mostly asymptomatic (42.9%) or complained of difficult dark adaptation (57.1%) (Fig 2). At the study visit, the mean BCVA of our cohort was 50.7 ± 22.0 ETDRS letters (20/100 Snellen equivalents, range: 10−85). However, meaningful differences were observed among phenotypes, with patients with CRD having the worst BCVA (28.8 ± 13.5 letters; all $P \leq 0.01$) and FFM group almost preserved vision (78.5 ± 10.5 letters; all $P \leq 0.01$).

Complete demographic and clinical characteristics are reported in Table 1.

Genotype-Phenotype Correlation

Overall, 54 different variants in the *ABCA4* gene were identified among the 132 alleles of our cohort, with 5 patients carrying homozygous variants (7.6%). Missense variants were the most common (86 alleles, 65.2%), followed by splice site variants (28 alleles, 21.2%). The most frequent mutations were the missense c.5882G>A with an allelic frequency of 26/132 (19.7%) and the splice site c.5714+5G>A (12/132, 9.1%). A list with the most frequently identified variants is available in Table S2 (available at www.ophthalmologyretina.org).

When evaluating the genotype-phenotype correlation, CD-BEM was significantly associated with the identification of missense variants ($P = 0.02$), and SD with structural variants ($P \leq 0.01$), whereas CRD and LO-SD phenotypes more frequently carried splice site variants ($P \leq 0.001$ and $P = 0.001$, respectively). Variants detected in patients with CRD were located more upstream in the *ABCA4* gene (median, exon 21 [12.3−30.0]) compared with LO-SD ($P = 0.04$). Of note, the hypomorphic c.5603A>T p.(Asn1868Ile) variant was found to be pathogenic in 2 patients affected by LO-SD in *trans* with nonsense variants, in 1 patient with FFM in *trans* with a missense variant, and 1 patient with CD-BEM in *trans* with a severe nonsense variant. The age at onset of patients carrying hypomorphic variants was significantly higher (54.8 ± 2.9 vs. 37.9 + 19.9 years; $P < 0.001$). An overview of the distribution of *ABCA4* variants across ABCA4R phenotypes is depicted in Figure 2.

Imaging Characterization of *ABCA4R* Phenotypes

Peripapillary sparing of the retina and RPE was detected using fundus autofluorescence in all eyes except for 3 (2.3%). These 3 eyes were all affected by LO-SD and exhibited advanced RPE atrophic changes (mean DDAF area: 25.8 ± 4.1 mm^2).

Signs of RPE atrophy were observed on blue autofluorescence in 98 eyes (74.2%), with a mean area of DDAF of 6.5 ± 9.0 mm^2. Retinal pigment epithelium atrophy was more frequent in eyes affected by CRD (10, 83.3%), SD (25, 89.3%), and LO-SD (38, 100%) (all $P < 0.05$). The extent of DDAF areas was significantly higher in patients with LO-SD (16.4 ± 10.8 mm^2) compared with other phenotypes (all $P < 0.001$). Areas of iORA were typically found on OCT in FFM eyes (14, 100%) ($P < 0.001$). Complete outer retinal atrophy was variably identified across all phenotypes, and was significantly more common in CD-BEM (39, 97.5%) and

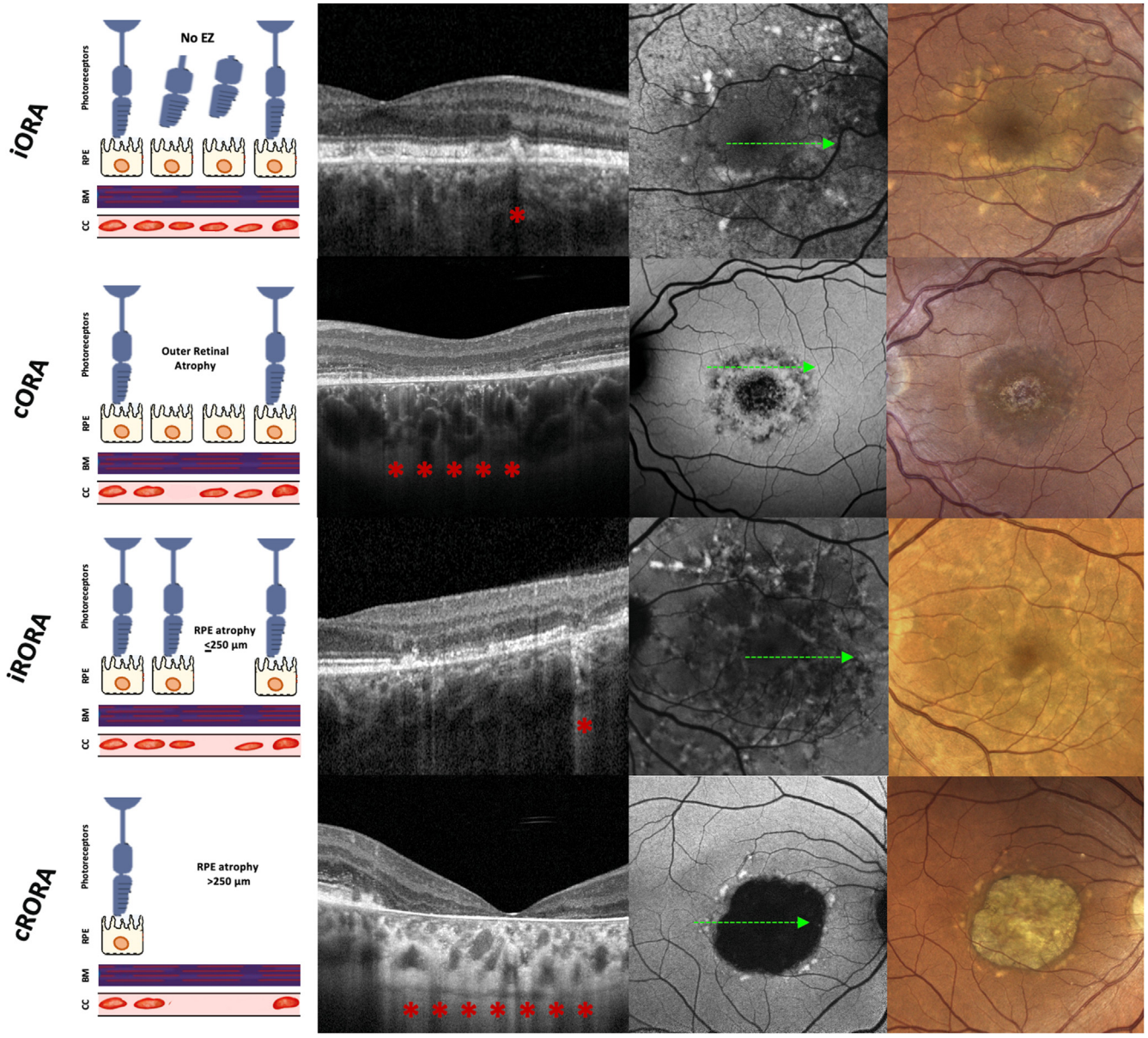

Figure 3. Graphical and imaging representation of the different atrophy types in *ABCA4*-associated retinopathies based on the recommendations of the Classification of Atrophy Meeting group. Small areas of incomplete outer retinal atrophy (iORA, red asterisk) are primarily observed in fundus flavimaculatus (FFM) over areas of flecks, with preservation of the overlying external limiting membrane. In contrast, complete outer retinal atrophy (cORA) is typically detected in the subfoveal area of *ABCA4*-related cone dystrophies (red asterisks), corresponding to regions of questionably decreased autofluorescence and altered foveal reflex on fundus photography. A few areas of incomplete retinal pigment epithelium (RPE) and outer retinal atrophy (iRORA, <250 µm) are present in cone dystrophy and FFM (red asterisk) but cannot be clearly visualized on autofluorescence and fundus photography. Lastly, complete RPE and outer retinal atrophy (cRORA, >250 µm) can be identified in the macula of a patient with Stargardt disease (red asterisks), corresponding to clear areas of RPE degeneration on fundus photography and of both questionably and definitely decreased autofluorescence. BM = Bruch's membrane; CC = choriocapillaris; EZ = ellipsoid zone.

patients with CRD (12, 100%) (both $P < 0.001$). The presence of incomplete RPE and outer retinal atrophy was more frequently observed in CD-BEM eyes (9, 22.5%) than other phenotypes ($P = 0.003$), whereas cRORA alterations were consistently associated with CRD (12, 100%) and LO-SD (38, 100%) (both $P < 0.001$). Representative cases of the different atrophy types are illustrated in Figure 3. Macular thickness analysis revealed that fovea was significantly thinner in CD-BEM (169 ± 43 µm), CRD (139 ± 34 µm), and SD eyes (166 ± 56 µm) compared with the other phenotypes (all $P < 0.05$). All phenotypes had reduced parafoveal thickness compared with patients with FFM (all P 0.001). On the other hand, the perifovea was preserved in both CD-BEM (268 ± 23 µm) and FFM eyes (290 ± 14 µm) (all $P < 0.05$).

The different patterns of flecks were variably distributed across phenotypes (P-value range: 0.001−0.56), with only 7 eyes affected by CD-BEM (17.5%) not showing any flecks. Although punctate

Table 3. Multimodal Imaging Differences across Phenotypes of *ABCA4* Retinopathies

	CD-BEM	CRD	SD	LO-SD	FFM
Peripapillary sparing					
Presence, n (%)	40 (100%)	12 (100%)	28 (100%)	35 (92%)	14 (100%)
RPE atrophy					
Presence, n (%)	25 (63%)	10 (83%)	25 (89%)	38 (100%)	0 (0%)
DDAF area, mm^2	1.0 ± 1.3	4.6 ± 3.8	5.1 ± 4.2	16.4 ± 10.8	0.0 ± 0.0
CAM atrophy types					
iORA, n (%)	1 (3%)	0 (0%)	0 (0%)	0 (0%)	14 (100%)
cORA, n (%)	39 (98%)	12 (100%)	20 (71%)	6 (16%)	2 (14%)
iRORA, n (%)	9 (23%)	0 (0%)	5 (18%)	0 (0%)	2 (14%)
cRORA, n (%)	18 (45%)	12 (100%)	23 (82%)	38 (100%)	0 (0%)
Macular thickness analysis					
CST, μm	169 ± 43	139 ± 34	166 ± 56	200 ± 62	291 ± 38
Parafovea, μm	240 ± 33	220 ± 17	215 ± 41	209 ± 48	318 ± 27
Perifovea, μm	268 ± 23	230 ± 28	258 ± 29	208 ± 46	291 ± 14
Flecks					
Presence, n (%)	33 (83%)	12 (100%)	28 (100%)	38 (100%)	14 (100%)
Punctate, n (%)	33 (83%)	12 (100%)	22 (79%)	31 (82%)	11 (79%)
Linear, n (%)	1 (3%)	2 (17%)	9 (32%)	19 (50%)	3 (21%)
Pisciform, n (%)	9 (23%)	12 (100%)	28 (100%)	31 (82%)	10 (71%)
Multiradiate, n (%)	1 (3%)	0 (0%)	8 (29%)	8 (21%)	4 (29%)
Resorbed, n (%)	9 (23%)	12 (100%)	18 (64%)	34 (89%)	8 (57%)
Choroidal structure					
CC flow deficit, $μm^2$	0.6 ± 0.6	1.1 ± 0.7	0.7 ± 0.5	2.7 ± 2.6	0.4 ± 0.3
SCT, μm	298 ± 108	330 ± 154	277 ± 103	179 ± 69	296 ± 68

CAM = Classification of Atrophy Meeting; CC = choriocapillaris; CD-BEM = cone dystrophy-bull's-eye maculopathy; cORA = complete outer retinal atrophy; CRD = cone-rod dystrophy; cRORA = complete RPE and outer retinal atrophy; CST = central subfield thickness; DDAF = definitely decreased autofluorescence; FFM = fundus flavimaculatus; iORA = incomplete outer retinal atrophy; iRORA = incomplete RPE and outer retinal atrophy; LO-SD = late-onset Stargardt disease; RPE = retinal pigment epithelium; SCT = subfoveal choroidal thickness; SD = Stargardt disease.

flecks were similarly distributed (79%−100%, $P = 0.55$), pisciform flecks were significantly associated with CRD and SD phenotypes (100%, both $P \leq 0.01$). Resorbed flecks occurred more frequently in CRD and LO-SD eyes (89%−100%; both $P < 0.01$) where the extent of DDAF area was significantly larger (8.4 ± 9.8 vs. 3.5 + 6.7 mm^2; $P = 0.002$). Patients with LO-SD also exhibited severe reduction of subfoveal choroidal thickness (179 ± 69 μm; all $P \leq 0.001$) and larger areas of flow deficits (2.7 ± 2.50 $μm^2$; all $P \leq 0.01$) with respect to other phenotypes. All imaging differences among phenotypes are reported in Table 3 and illustrated in Figure 4.

Repeatability Analysis

Interobserver agreement was excellent for all the analyzed variables (intraclass correlation coefficient = 0.899, [0.809−0.989] and $k = 0.93$, [0.87−0.98]). However, Bland−Altman plots highlighted lower repeatability for the measurement of DDAF areas in phenotypes other than LO-SD, particularly for small RPE atrophic areas (Fig 5). In contrast, the agreement for the grading of complete outer retinal atrophy (90%−100%) and cRORA (89%−100%) was very high across all phenotypes.

Discussion

Several therapeutic approaches are currently being pursued for autosomal recessive retinal dystrophies including cell-based, gene augmentation, and drug therapies.[28] Although *ABCA4*-associated retinal dystrophies represent an attractive candidate,[29] accurate phenotyping and definition of clinical end points remain challenging — this impacts the ability to evaluate therapeutic benefits. *ABCA4* retinopathies pose additional challenges due to their heterogeneity,[4] and the identification of > 2300 disease-causing variants in the *ABCA4* gene renders the correlation between genotypic and phenotypic features even more complicated.

To accommodate this problem, Lambertus et al[15] proposed a composite model for early-onset SD based on multimodal imaging measurements. This sensitive model, however, did not take into consideration the large variability observable in the spectrum of *ABCA4*-associated retinal degeneration; thus, a comprehensive characterization of the *ABCA4* retinopathies is required. Several classifications and possible outcome measures have been proposed in literature and some have been adopted in clinical trials.[5,7−10] In our cross sectional research, we presented deep phenotyping data on 66 patients affected by ABCA4R. We identified 5 distinct clinical phenotypes based on age at onset, imaging features, and ERG alterations and highlighted the differences between these phenotypes to speculate on their pathogenesis and select potential clinical end points.

Age at presentation can be largely heterogeneous across phenotypes, as previously reported.[8,30,31] Of notice, patients with CRD were the youngest (mean age of 14 years); a bimodal distribution was observed in CD-BEM phenotype with a first peak around 20 years of age and a second in their 40s to 50s. This bimodal behavior can be presumably

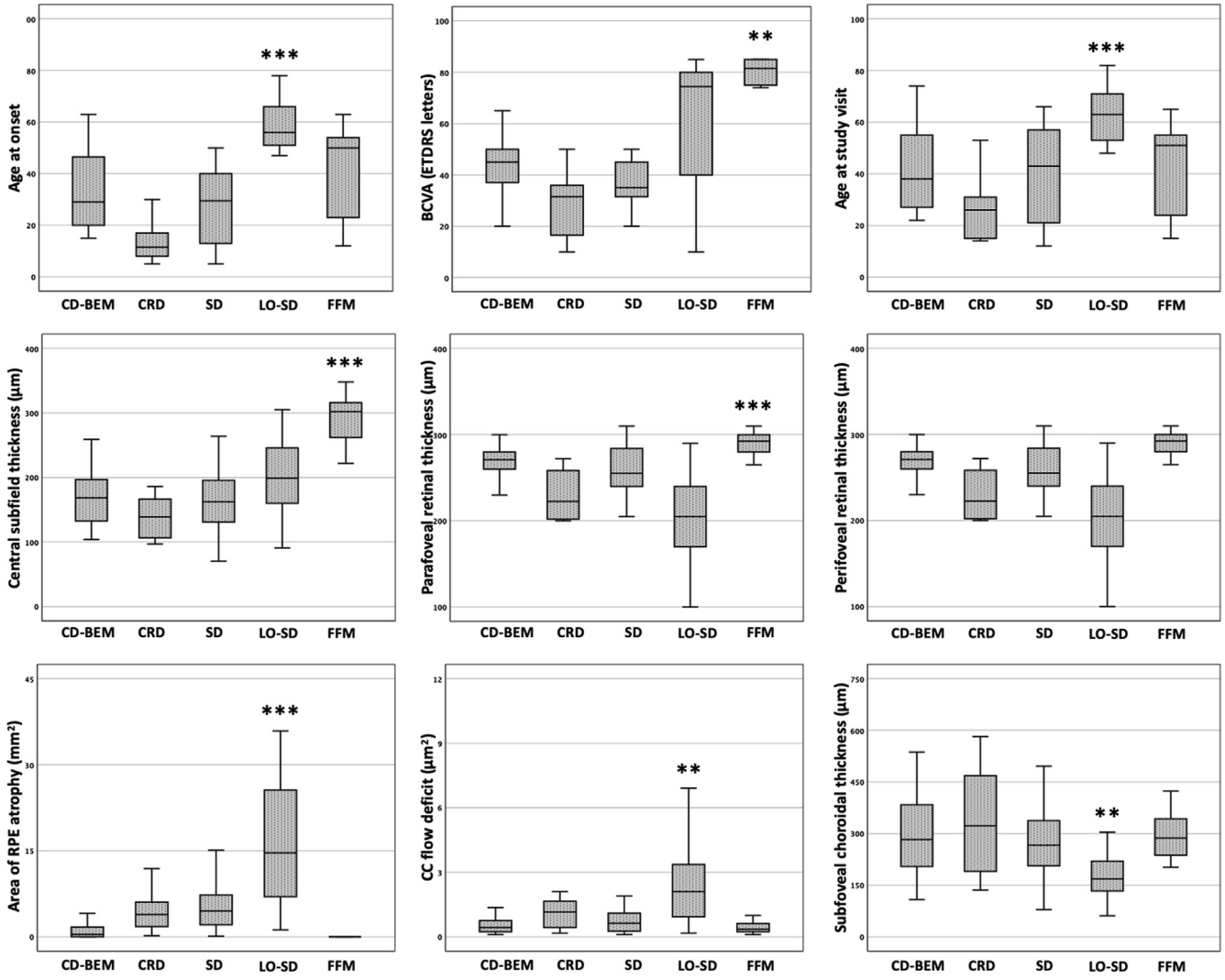

Figure 4. Differences in age, visual acuity, and retinal and choroidal alterations across the different phenotypes. Patients affected by late-onset Stargardt disease (LO-SD) have an older age and more extensive areas of retinal pigment epithelium (RPE) atrophy and choroidal changes compared with the other phenotypes. Patients with fundus flavimaculatus (FFM), on the other hand, have better visual acuity and preserved macular thickness (*$P < 0.05$; **$P < 0.01$; ***$P < 0.001$). BCVA = best-corrected visual acuity; CC = choriocapillaris; CD-BEM = cone dystrophy-bull's-eye maculopathy; CRD = cone-rod dystrophy.

ascribed to the interaction between 2 affected alleles with hypomorphic variants leading to a later onset of the disease.[32] Presenting symptoms were also highly variable, with patients with an early onset (e.g., CD-BEM and CRD) more frequently complaining of central vision loss and photosensitivity. These symptoms were rarely reported by patients with LO-SD, who showed better central vision owing to foveal sparing but complained of progressive difficulty in activities conducted under dim-light conditions due to the wide areas of macular RPE degeneration.[33]

Best-corrected visual acuity measurement is not considered a reliable outcome measure in ABCA4R, as it is strictly dependent on foveal involvement.[34] In contrast with other macular dystrophies, pediatric and young patients with ABCA4R have worse central vision.[35,36] This feature was typical of severe (e.g., CRD) or early fovea-involving (e.g., CD-BEM) phenotypes. Conversely, patients affected by FFM had an overall good presentation with preserved central vision or initial dark adaptation problems.

The genetic mechanisms behind the phenotypic heterogeneity of ABCA4Rs remain elusive,[16] and a thorough assessment of possible genetic modifiers with *in silico* cross-validations is certainly warranted.[29] Missense variants were the most common in our cohort and were significantly associated with CD-BEM phenotype. This is consistent with other reports, where single nucleotide substitutions are associated with relatively benign presentations.[37] Of note, the most frequent hypomorphic variant (c.5603A>T p.Asn1868Ile) was also found in 1 patient affected by CD-BEM with late disease onset (>45 years). Splice site variants were similarly distributed across different phenotypes, such as CRD and LO-SD. This might be explained by the location of genetic mutations, as the majority of patients with CRD carried disease-causing

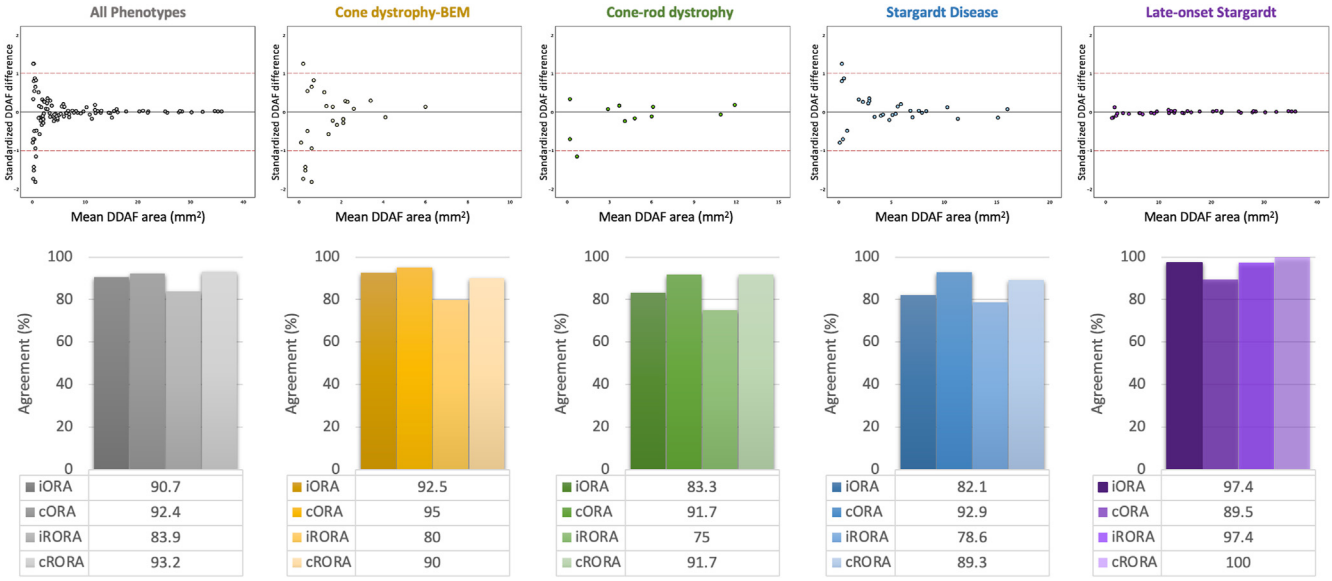

Figure 5. Bland–Altman plots and bar charts showing the repeatability of the analyzed variables. Lower repeatability for definitely decreased autofluorescence (DDAF) can be observed for small areas of retinal pigment epithelium atrophy (RPE) and for phenotypes with mixed photoreceptor-RPE degeneration (e.g., cone and cone-rod dystrophies). BEM = bull's-eye maculopathy; cORA = complete outer retinal atrophy; cRORA = complete retinal pigment epithelium and outer retinal atrophy; iORA = incomplete outer retinal atrophy; iRORA = incomplete retinal pigment epithelium and outer retinal atrophy.

mutations in more upstream regions of *ABCA4* gene, thus leading to null alleles and more severe alterations.

Numerous clinical studies have investigated the imaging characteristics of ABCA4Rs.[4,6,12,16] Peripapillary sparing is typically considered a diagnostic feature in these patients.[38] Involvement of this area was rarely described in severe cases characterized by cone-rod dysfunction on electrophysiology.[39] The reason for peripapillary resilience to *ABCA4* gene mutations remains unclear; theories suggest the presence of a more favorable photoreceptor:RPE ratio, a reduced lipofuscin build-up, and phototoxicity due to a thicker overlying retinal nerve fiber layer.[38]

Our data are consistent with those of Burke et al,[39] suggesting that the peripapillary involvement occurs more frequently in severe chorioretinal degeneration. Our series identified peripapillary involvement in 3 eyes affected by LO-SD: we hypothesize that the severe CC damage may play a significant role in peripapillary involvement and represent a distinctive feature.

The size of RPE atrophy and the repeatability of its measurement were significantly higher in patients with LO-SD compared with phenotypes featuring predominant photoreceptor alterations (e.g., CD-BEM and CRD) and small RPE atrophic changes (Fig 5): the autofluorescence resulting from photoreceptor degeneration and flecks reabsorption might in fact affect the assessment of DDAF in these phenotypes.[9] Complete outer retinal atrophy alterations were also more commonly observed in these phenotypes, whereas cRORA were more frequently identified in patients with LO-SD. These data have important implications for the selection of clinical end points. Specifically, the quantification of DDAF seems a reliable outcome measure in LO-SD, whereas other phenotypes characterized by preferential photoreceptor involvement and variable RPE atrophy might benefit from different outcome measures, such as ellipsoid zone disruption and outer nuclear layer thickness.[10] In this regard, macular thickness analysis showed a significant reduction of parafoveal thickness in all phenotypes except for FFM, thus suggesting that the middle ETDRS ring might be the most sensitive when considering phenotypes altogether.

Flecks are also considered an important diagnostic element in ABCA4R — albeit not pathognomonic[40] — which can be detected at baseline or may develop at some point during follow-up.[4] In our series, only 7 eyes did not show signs of flecks and were all classified in the CD-BEM group.

The higher prevalence of resorbed flecks in CRD and LO-SD seemed to correlate with more profound alterations at the level of the RPE and CC in their progression toward RPE atrophy. This phenotypic heterogeneity reinforces the hypothesis that flecks distribution might reflect different disease stages or pathogenic mechanisms,[41] such as severe photoreceptor damage or preferential RPE involvement deriving from CC impairment.

Lastly, CC alterations as detectable on OCTA are gaining further consideration as potential biomarkers due to the continuous improvement in quantitative metrics.[27] Previous studies have identified distinct features of CC alterations compared with age-related macular degeneration.[12,42] Our report confirms that a significant impairment of the inner choroid can be observed outside areas of RPE atrophy, particularly in LO-SD.

Limitations of this study to be addressed in future works include its cross sectional design and therefore the absence of longitudinal data and the lack of functional data other than

BCVA. The limited sample size of some phenotypes might have attenuated statistical significance for some of the analyzed variables. Moreover, choroidal vascular alterations were assessed using novel OCTA metrics (flow deficit) and were not compared with indocyanine green angiography findings.[43] Further research is warranted to assess their natural history and establish any possible crosstalk between phenotypes.

In conclusion, this report explored the clinical and imaging characteristics in the phenotypic spectrum of *ABCA4*-associated retinal dystrophies. Our findings suggest that different photoreceptor and RPE layer involvement may contribute to these characteristics, with a possible role played by CC impairment. Based on our results, it is recommended that clinical end points for *ABCA4*-associated retinal dystrophies be differentiated according to the structural features within each phenotype, as current outcome measures may not be repeatable for some stages or presentations of ABCA4Rs.

Footnotes and Disclosures

Originally received: May 14, 2023.
Final revision: October 18, 2023.
Accepted: October 24, 2023.
Available online: November 3, 2023. Manuscript no. ORET-D-23-00313R1.

[1] Eye Clinic, Department of Biomedical and Clinical Science, Luigi Sacco Hospital, University of Milan, Milan, Italy.

[2] Harvard Retinal Imaging Lab, Retina Service, Department of Ophthalmology, Massachusetts Eye and Ear, Boston, Massachusetts.

[3] Department of Ophthalmology, Leiden University Medical Center, Leiden, The Netherlands.

[4] Department of Ophthalmology, Amsterdam University Medical Center, Amsterdam, The Netherlands.

[5] Cole Eye Institute, Cleveland Clinic, Cleveland, Ohio.

[6] Eye Institute, Cleveland Clinic, Abu Dhabi, United Arab Emirates.

[7] MAGI Group, San Felice del Benaco, Italy.

[8] Department of Ophthalmology, Save Sight Institute, University of Sydney, Sydney, Australia.

Disclosure(s):

All authors have completed and submitted the ICMJE disclosures form.

The author(s) have made the following disclosures: G.S.: Consultant − Heidelberg Engineering, Optos, Optovue, CenterVue, Allergan, Bayer, Genetech, Novartis, Quantel Medical, Carl Zeiss Meditec, Boehringer, Topcon, and Roche.

A.I.: Consultant − Novartis and Bayer; Recipient − Allergan.

The other authors have no proprietary or commercial interest in any materials discussed in this article.

HUMAN SUBJECTS: Human subjects were included in this study. The procedures adhered to the tenets of the Declaration of Helsinki, and all patients were enrolled after approval by the institutional review board of Ospedale Luigi Sacco. Written informed consent was obtained from each participant after explaining the study protocol.

No animal subjects were used in this study.

Author Contributions:

Conception and design: Romano, Lamanna, Boon, Siligato, Kalra, Agarwal, Medori, Bertelli, Pellegrini, Invernizzi, Staurenghi, Salvetti

Data collection: Romano, Lamanna, Boon, Siligato, Kalra, Agarwal, Medori, Bertelli, Pellegrini, Invernizzi, Staurenghi, Salvetti

Analysis and interpretation: Romano, Lamanna, Boon, Siligato, Kalra, Agarwal, Medori, Bertelli, Pellegrini, Invernizzi, Staurenghi, Salvetti

Obtained funding: N/A

Overall responsibility: Romano, Lamanna, Boon, Siligato, Kalra, Agarwal, Medori, Bertelli, Pellegrini, Invernizzi, Staurenghi, Salvetti

Abbreviations and Acronyms:
ABCA4R = *ABCA4*-related retinopathy; **BCVA** = best-corrected visual acuity; **CC** = choriocapillaris; **CD-BEM** = cone dystrophy-bull's-eye maculopathy; **CRD** = cone-rod dystrophy; **cRORA** = complete retinal pigment epithelium and outer retinal atrophy; **DDAF** = definitely decreased autofluorescence; **ERG** = electroretinogram; **FFM** = fundus flavimaculatus; **LO-SD** = late-onset Stargardt disease; **OCTA** = OCT angiography; **RPE** = retinal pigment epithelium; **SD** = Stargardt disease.

Keywords:
ABCA4 retinopathy, End points, Multimodal imaging, Phenotypes, Stargardt.

Correspondence:
Francesco Romano, MD, Eye Clinic, Department of Biomedical and Clinical Science, Luigi Sacco Hospital, University of Milan, Via G.B. Grassi, 74 − 20157, Milan, Italy. E-mail: fromano1@meei.harvard.edu.

References

1. Spiteri Cornish K, Ho J, Downes S, et al. The epidemiology of Stargardt disease in the United Kingdom. *Ophthalmol Retina*. 2017;1:508−513.
2. Al-Khuzaei S, Shah M, Foster CR, et al. The role of multimodal imaging and vision function testing in ABCA4-related retinopathies and their relevance to future therapeutic interventions. *Ther Adv Ophthalmol*. 2021;13:25158414211056384.
3. Allikmets R, Singh N, Sun H, et al. A photoreceptor cell-specific ATP-binding transporter gene (ABCR) is mutated in recessive Stargardt macular dystrophy. *Nat Genet*. 1997;15:236−246.
4. Sparrow JR, Gregory-Roberts E, Yamamoto K, et al. The bisretinoids of retinal pigment epithelium. *Prog Retin Eye Res*. 2012;31:121−135.
5. Fishman GA. Fundus flavimaculatus. A clinical classification. *Arch Ophthalmol*. 1976;94:2061−2067.
6. Arrigo A, Grazioli A, Romano F, et al. Multimodal evaluation of central and peripheral alterations in Stargardt disease: a pilot study. *Br J Ophthalmol*. 2020;104:1234−1238.
7. Fujinami K, Lois N, Mukherjee R, et al. A longitudinal study of Stargardt disease: quantitative assessment of fundus autofluorescence, progression, and genotype correlations. *Invest Ophthalmol Vis Sci*. 2013;54:8181−8190.
8. Lois N, Holder GE, Bunce C, et al. Phenotypic subtypes of Stargardt macular dystrophy-fundus flavimaculatus. *Arch Ophthalmol*. 2001;119:359−369.
9. Strauss RW, Muñoz B, Ho A, et al. ProgStar study. Progression of Stargardt disease as determined by fundus autofluorescence in the retrospective progression of Stargardt

disease study (ProgStar Report No. 9). *JAMA Ophthalmol*. 2017;135:1232−1241.
10. Pfau M, Cukras CA, Huryn LA, et al. Photoreceptor degeneration in ABCA4-associated retinopathy and its genetic correlates. *JCI Insight*. 2022;7:e155373.
11. Müller PL, Gliem M, McGuinnes M, et al. Quantitative fundus autofluorescence in ABCA4-related retinopathy - functional relevance and genotype-phenotype correlation. *Am J Ophthalmol*. 2021;222:340−350.
12. Pellegrini M, Acquistapace A, Oldani M, et al. Dark atrophy: an optical coherence tomography angiography study. *Ophthalmology*. 2016;123:1879−1886.
13. Battaglia Parodi M, Sacconi R, Romano F, Bandello F. Hyperreflective foci in Stargardt disease: 1-year follow-up. *Graefes Arch Clin Exp Ophthalmol*. 2019;257:41−48.
14. Arrigo A, Romano F, Aragona E, et al. OCTA-based identification of different vascular patterns in Stargardt disease. *Transl Vis Sci Technol*. 2019;8:26.
15. Lambertus S, Bax NM, Fakin A, et al. Highly sensitive measurements of disease progression in rare disorders: developing and validating a multimodal model of retinal degeneration in Stargardt disease. *PLOS ONE*. 2017;12:e0174020.
16. Cremers FPM, Lee W, Collin RWJ, Allikmets R. Clinical spectrum, genetic complexity and therapeutic approaches for retinal disease caused by ABCA4 mutations. *Prog Retin Eye Res*. 2020;79:100861.
17. Romano F, Airaldi M, Cozzi M, et al. Progression of atrophy and visual outcomes in extensive macular atrophy with pseudodrusen-like appearance. *Ophthalmol Sci*. 2021;1:1−10.
18. Richards S, Aziz N, Bale S, et al. Standards and guidelines for the interpretation of sequence variants: a joint consensus recommendation of the American College of Medical Genetics and Genomics and the Association for Molecular Pathology. *Genet Med*. 2015;17:405−424.
19. Michaelides M, Chen LL, Brantley Jr MA, et al. ABCA4 mutations and discordant ABCA4 alleles in patients and siblings with bull's-eye maculopathy. *Br J Ophthalmol*. 2007;91:1650−1655.
20. Hamel CP. Cone rod dystrophies. *Orphanet J Rare Dis*. 2007;2:7.
21. Lambertus S, Lindner M, Bax NM, et al. Progression of late-onset Stargardt disease. *Invest Ophthalmol Vis Sci*. 2016;57:5186−5191.
22. Franceschetti A. A special form of tapetoretinal degeneration: fundus flavimaculatus. *Trans Am Acad Ophthalmol Otolaryngol*. 1965;69:1048−1053.
23. Strauss RW, Kong X, Ho A, et al. Progression of Stargardt disease as determined by fundus autofluorescence over a 12-month period: ProgStar Report No. 11. *JAMA Ophthalmol*. 2019;137:1134−1145.
24. Guymer RH, Rosenfeld PJ, Curcio CA, et al. Incomplete retinal pigment epithelial and outer retinal atrophy in age-related macular degeneration: classification of atrophy meeting report 4. *Ophthalmology*. 2020;127:394−409.
25. Rahman W, Chen FK, Yeoh J. Repeatability of manual subfoveal choroidal thickness measurements in healthy subjects using the technique of enhanced depth imaging optical coherence tomography. *Invest Ophthalmol Vis Sci*. 2011;52:2267e2271.
26. Chu Z, Cheng Y, Zhang Q, et al. Quantification of choriocapillaris with phansalkar local thresholding: pitfalls to avoid. *Am J Ophthalmol*. 2020;213:161−176.
27. Chu Z, Zhang Q, Gregori G, et al. Guidelines for imaging the choriocapillaris using OCT angiography. *Am J Ophthalmol*. 2021;222:92−101.
28. Tanna P, Strauss RW, Fujinami K, Michaelides M. Stargardt disease: clinical features, molecular genetics, animal models and therapeutic options. *Br J Ophthalmol*. 2017;101:25−30.
29. Al-Khuzaei S, Broadgate S, Foster CR, et al. An overview of the genetics of ABCA4 retinopathies, an evolving story. *Genes (Basel)*. 2021;12:1241.
30. Lambertus S, van Huet RA, Bax NM, et al. Early-onset Stargardt disease: phenotypic and genotypic characteristics. *Ophthalmology*. 2015;122:335−344.
31. Westeneng-van Haaften SC, Boon CJ, Cremers FP, et al. Clinical and genetic characteristics of late-onset Stargardt's disease. *Ophthalmology*. 2012;119:1199−1210.
32. Bauwens M, Garanto A, Sangermano R, et al. ABCA4-associated disease as a model for missing heritability in autosomal recessive disorders: novel noncoding splice, cis-regulatory, structural, and recurrent hypomorphic variants. *Genet Med*. 2019;21:1761−1771.
33. van Huet RA, Bax NM, Westeneng-Van Haaften SC, et al. Foveal sparing in Stargardt disease. *Invest Ophthalmol Vis Sci*. 2014;55:7467−7478.
34. Rotenstreich Y, Fishman GA, Anderson RJ. Visual acuity loss and clinical observations in a large series of patients with Stargardt disease. *Ophthalmology*. 2003;110:1151−1158.
35. Battaglia Parodi M, Romano F, Arrigo A, et al. Natural course of the vitelliform stage in best vitelliform macular dystrophy: a five-year follow-up study. *Graefes Arch Clin Exp Ophthalmol*. 2020;258:297−301.
36. Boon CJ, Klevering BJ, Cremers FP, et al. Central areolar choroidal dystrophy. *Ophthalmology*. 2009;116:771−782, 782.e1.
37. Maugeri A, van Driel MA, van de Pol DJ, et al. The 2588G−>C mutation in the ABCR gene is a mild frequent founder mutation in the Western European population and allows the classification of ABCR mutations in patients with Stargardt disease. *Am J Hum Genet*. 1999;64:1024−1035.
38. Cideciyan AV, Swider M, Aleman TS, et al. ABCA4-associated retinal degenerations spare structure and function of the human parapapillary retina. *Invest Ophthalmol Vis Sci*. 2005;46:4739−4746.
39. Burke TR, Rhee DW, Smith RT, et al. Quantification of peripapillary sparing and macular involvement in Stargardt disease (STGD1). *Invest Ophthalmol Vis Sci*. 2011;52:8006−8015.
40. Boon CJ, van Schooneveld MJ, den Hollander AI, et al. Mutations in the peripherin/RDS gene are an important cause of multifocal pattern dystrophy simulating STGD1/fundus flavimaculatus. *Br J Ophthalmol*. 2007;91:1504−1511.
41. Cukras CA, Wong WT, Caruso R, et al. Centrifugal expansion of fundus autofluorescence patterns in Stargardt disease over time. *Arch Ophthalmol*. 2012;130:171−179.
42. Müller PL, Pfau M, Möller PT, et al. Choroidal flow signal in late-onset Stargardt disease and age-related macular degeneration: an OCT-angiography study. *Invest Ophthalmol Vis Sci*. 2018;59:AMD122−AMD131.
43. Giani A, Pellegrini M, Carini E, et al. The dark atrophy with indocyanine green angiography in Stargardt disease. *Invest Ophthalmol Vis Sci*. 2012;53:3999−4004.